which is identical to eq.(3.177) when the therm $\mathbf{s}^{i+1}$ is dropped. Notice, however, that this term couldn't simply be dropped from the above-mentioned equation on the basis that the said term vanishes, because the structural error is not expected to vanish at the optimum solution. The computation of $\Delta\mathbf{k}^i$ from eq.(3.180) now should be pursued via an orthogonalization procedure, as studied in Subsection 1.4.5. With $\Delta\mathbf{k}^i$ calculated, the ith iteration is complete, as a new, improved value $\mathbf{k}^{i+1}$ of the design parameter vector $\mathbf{k}$ is available. Now the new structural-error vector value $\mathbf{s}^{i+1}$ can be computed, and then the normality condition verified. If the condition is not verified, a new iteration is in order; if the same condition is verified, then the procedure stops. An alternative convergence criterion, equivalent to the latter, is to verify whether $\|\Delta\mathbf{k}^i\| < \epsilon$, for a prescribed tolerance ϵ. The equivalence of the two criteria should be apparent from the relation between $\Delta\mathbf{k}^i$ and the product of the last three factors of the right-hand side of eq.(3.179).

Branch-switching Detection

This Subsubsection is limited to planar linkages, its generalization to spherical and spatial linkages should be doable, as the problem under study is based on the concept of the sign of the transmission index. The latter was studied in Section 3.6.

In the foregoing analysis an implicit assumption was adopted: all generated values $\{\,\phi_i\,\}_1^m$ lie on the same linkage branch. However, all four-bar linkages studied in this chapter, planar, spherical and spatial, were shown in Section 3.4 to be *bimodal*, i.e., they all entail two solution branches of their input-output equation. This means that, within an iteration loop, the occurrence of branch-switching should be monitored. Below we explain a simple means of doing this, as applicable to planar linkages. The two branches of a typical planar four-bar linkage are apparent in Fig. 3.8(a). In this figure, the transmission angle is $\mu = \angle BCD$ in one branch, in the second being $\mu' = \angle BC'D$. The qualitative difference between the two branches lies in *the sign of the sine of the transmission angle*, for, in the first branch, we have $\sin\mu > 0$; in the second, $\sin\mu' < 0$. Moreover, $\sin\mu$ vanishes at *deadpoints*, when the input angle reaches either a maximum or a minimum—linkages of this kind have an input rocker. Hence, a simple way of deciding whether all values $\{\,\phi_i\,\}_1^m$ lie in the same branch relies on the computation of $\sin\mu$ with the correct sign. This is most simply done by means of the 2D version of the cross product[12] of vectors $\overrightarrow{CB} = \mathbf{b} - \mathbf{c}$ and $\overrightarrow{CD} = \mathbf{d} - \mathbf{c}$, in this order, where $\mathbf{b}$, $\mathbf{c}$ and $\mathbf{d}$ are the position vectors of points B, C and D, respectively, in the given coordinate frame. The product at stake is given by

$$p \equiv (\mathbf{b}-\mathbf{c})^T\mathbf{E}(\mathbf{d}-\mathbf{c}) = \|\mathbf{b}-\mathbf{c}\|\|\mathbf{d}-\mathbf{c}\|\sin\mu = a_3a_4\sin\mu \tag{3.181}$$

[12]See Subsection 1.4.1.

with **E** introduced in eq.(1.1a). Given that the link lengths are positive, we have the relation

$$\text{sgn}(\sin\mu) = \text{sgn}(p) \tag{3.182}$$

which now can be used to monitor branch-switching.

Introducing a Massive Number of Data Points

As shown by Hayes et al. (1999), one simple way of minimizing the structural error is via design-error minimization *in the presence of a large number of prescribed poses*. We show with one example below that, as the cardinality m of the data set increases, the design and structural errors converge. The results are taken from the foregoing reference.

In the example below, the *weighted Euclidean norm* of the design and the structural error, $\|\mathbf{e}\|_{2W}$ and $\|\mathbf{s}\|_{2W}$, respectively, are minimized. For any m-dimensional vector $\mathbf{v}$, this norm is defined as the rms value of its components, namely,

$$\|\mathbf{v}\|_{2W} \equiv \sqrt{\frac{1}{m}\mathbf{v}^T\mathbf{v}} \tag{3.183}$$

Example 3.7.1 *We synthesize here a planar and a spherical RRRR four-bar linkage to generate a quadratic I/O function for the values given below:*

$$\psi_i = \alpha + \Delta\psi_i,\ \phi_i = \beta + \Delta\phi_i,\ \Delta\phi_i = \frac{9\Delta\psi_i^2}{8\pi},\ i = 1, \ldots, m$$

For each linkage the I/O dial zeros (α and β) are selected to minimize the condition number κ of **S** *for each data-set, in following the procedure proposed by Liu and Angeles (1993). Then both the design and structural errors are determined for the linkages that minimize the respective Euclidean norms for data-sets with cardinalities of $m = \{10, 40, 70,$ and $100\}$. These results are listed in Tables 3.5–3.8. Finally the structural errors, corresponding to $m = 40$, of the linkages that minimize the Euclidean norms of the design and structural errors are graphically displayed in Fig. 3.20.*

Table 3.5: Results for $m = 10$.

	Planar RRRR	Spherical RRRR
α_{opt} (°)	123.8668	43.3182
β_{opt} (°)	91.7157	89.5221
κ_{opt}	33.2974	200.5262
$\|\mathbf{e}\|_{2W}$	2.2999×10^{-3}	2.4033×10^{-4}
$\|\mathbf{s}\|_{2W}$	1.8863×10^{-3}	1.3187×10^{-4}

Table 3.6: Results for $m = 40$.

	Planar RRRR	Spherical RRRR
α_{opt} (°)	117.4593	42.7696
β_{opt} (°)	89.4020	88.8964
κ_{opt}	32.5549	203.0317
$\|\mathbf{e}\|_{2W}$	2.484×10^{-3}	2.984×10^{-4}
$\|\mathbf{s}\|_{2W}$	2.375×10^{-3}	1.671×10^{-4}

Table 3.7: Results for $m = 70$.

	Planar RRRR	Spherical RRRR
α_{opt} (°)	116.4699	42.7014
β_{opt} (°)	89.0488	88.8045
κ_{opt}	32.5242	204.7696
$\|\mathbf{e}\|_{2W}$	2.496×10^{-3}	3.031×10^{-4}
$\|\mathbf{s}\|_{2W}$	2.438×10^{-3}	1.701×10^{-4}

3.8 Synthesis Under Mobility Constraints

Read (Liu and Angeles, 1992).

3.9 Synthesis of Complex Linkages

To come.

3.9.1 Synthesis of Stephenson Linkages

To come.

Table 3.8: Results for $m = 100$.

	Planar RRRR	Spherical RRRR
α_{opt} (°)	116.0679	42.6740
β_{opt} (°)	88.9057	88.7674
κ_{opt}	32.5170	205.5603
$\|\mathbf{e}\|_{2W}$	2.499×10^{-3}	3.047×10^{-4}
$\|\mathbf{s}\|_{2W}$	2.464×10^{-3}	1.712×10^{-4}

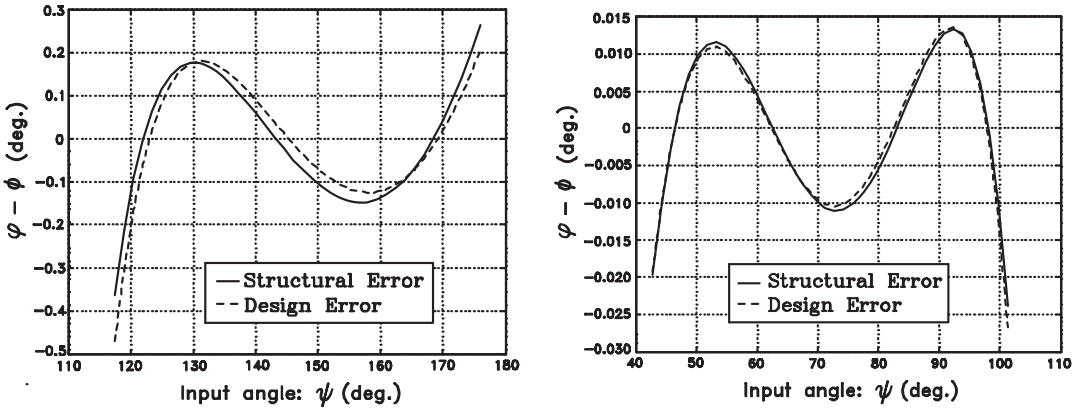

(a) (b)

Figure 3.20: Structural error comparison for: (a) planar and (b) spherical RRRR linkages upon minimizing $\|\mathbf{s}\|_{2W}$ & $\|\mathbf{e}\|_{2W}$.